



A novel strategy to fabricate thin film nanocomposite reverse osmosis membranes with enhanced desalination performance

Dapeng Zhang¹, Zicheng Yao¹, Han Zhang, Guiru Zhu*, Lu Liu, Congjie Gao

College of Chemistry and Chemical Engineering, Ocean University of China, Qingdao 266100, China, Tel. +86-0532-66782552, email: zdp19901023@qq.com (D.P. Zhang), 549635155@qq.com (Z.C. Yao), 837001493@qq.com (H. Zhang), zhugr@ouc.edu.cn (G.R. Zhu), 742881266@qq.com (L. Liu), gaocjie@ouc.edu.cn (C.J. Gao)

Received 18 June 2018; Accepted 28 December 2018

ABSTRACT

A novel strategy to fabricate thin film nanocomposite (TFN) membrane was reported by dispersing nanofillers in the aqueous and organic phase simultaneously via interfacial polymerization of *m*-phenylenediamine and trimesoyl chloride. Two different nanofillers (hydrophilic MCM-48 and hydrophobic ZIF-8) were used to investigate the new strategy. Both hydrophilic MCM-48 and hydrophobic ZIF-8 can effectively improve the separation performance of the TFN membrane with higher water flux value maintaining high salt rejection via the novel strategy than conventional TFN membrane prepared with same total amount nanoparticles in singly organic phase or aqueous phase. It indicates that the new strategy is feasible to obtain the TFN membrane with excellence separation performance compared with the conventional method by dispersing nanofillers in singly phase. The new strategy is realized by dispersing less amount nanofillers in both phases simultaneously, which is possible to avoid the aggregation of nanoparticles and maximize the effect of nanoparticles.

Keywords: Reverse osmosis membranes; Thin film nanocomposite; Interfacial polymerization; Nanofiller; Polyamide

1. Introduction

Globally, the water scarcity is a long-term serious challenge for human society. Currently, reverse osmosis (RO) membrane process dominates the global desalination market because of its simple operation and relatively lower energy consumption [1]. In order to reduce water cost, researchers pay great attentions to improve the separation performance of RO membrane, mainly to increase permeability and fouling-resistant. Jeong and his co-workers reported a thin film nanocomposite (TFN) membrane prepared via interfacial polymerization process by embedding zeolite nanoparticles in the polyamide thin film layer [2]. The water flux of the TFN RO membranes significantly increased without obviously decrease in salt rejection. Since then, the TFN membrane has been attracted broad attentions. In addition to zeolite [3–5], other nanomaterials have been used as nanofillers, such as hydrophilic or hydro-

phobic nanoparticles [6–13] and nanotubes [14–17]. All prepared TFN membranes showed improved separation performance, especially higher water flux. Some researchers found that TFN membranes possess anti-fouling properties attributing to the high hydrophilicity [12,13,17,18]. Therefore, the TFN membrane with higher water flux and fouling-resistant will reduce the water cost of desalination. However, the reported researches of the TFN membranes just focus on the influence of different nanofillers on the separation performance. The formation procedure of the reported TFN membranes are similar, that the nanomaterials were totally dispersed into aqueous phase or organic phase singly. For the reported TFN membranes, a similar phenomenon was found that the water flux increased progressively and the salt rejection decreased progressively with increasing nanofillers loading. However, the remarkable increase of water flux and remarkable decrease of salt rejection would be observed when larger amount of the nanofillers were added. It is believed that nanofillers aggre-

*Corresponding author.

¹Co-first authors

gation will be occurred at higher concentration, and large pores are likely to form between the aggregation nanoparticles, resulting in reduction of salt rejection and increase of water flux [17]. Therefore, the improved performance of the TFN membranes are limited under the current preparation process. Our previously studies showed that the nanofillers were embedded throughout the polyamide layer by dispersing in organic solution, while the same nanofillers were clipped between the polysulfone support and polyamide layer by dispersing in aqueous solution [19]. And, the two types of TFN membranes both exhibit higher water flux and enhanced long-term durability, confirming that same nanoparticles could improve the separation performance and are stable in the resultant TFN membranes with dispersed whether in organic phase or in aqueous phase. Therefore, it is feasible to disperse the same nanofillers in aqueous phase and organic phase simultaneously to fabricate the TFN membranes. To the best of our knowledge, the new strategy of preparing the TFN RO membrane by dispersing nanofillers in the two phases simultaneously of interfacial polymerization has never been reported.

Herein, we report a novel strategy to fabricate the TFN membranes by dispersing different nanoparticles (hydrophilic MCM-48 and hydrophobic ZIF-8) in the organic phase and aqueous phase simultaneously via interfacial polymerization of trimesoyl chloride (TMC) and *m*-phenylenediamine (MPD). The effect of different concentration and addition mode of nanoparticles on the desalination performance, chlorine resistance and stability properties of the novel TFN membranes was studied.

2. Experimental

2.1. Materials

Tetraethyl orthosilicate (TEOS) and cetyltrimethyl ammonium bromide (CTAB) were both purchased from Aladdin. Ammonium hydroxide (NH_4OH), ethanol and *n*-hexane were purchased from Sinopharm Chemical Reagent Co. Ltd. Triblock copolymer F127 ($\text{EO}_{106}\text{PO}_{70}\text{EO}_{106}$), zinc nitrate hexahydrate ($\text{Zn}(\text{NO}_3)_2 \cdot 6\text{H}_2\text{O}$), 2-methylimidazole, *m*-Phenylenediamine (MPD) and sodium dodecylsulfate (SDS) were purchased from Sigma-Aldrich. Trimesoyl chloride (TMC) was purchased from TCI. Polysulfone ultrafiltration membrane as a support was purchased from Hangzhou Water Treatment Center (Hangzhou China). All the chemicals are used as received.

2.2. Preparation of nanoparticles

MCM-48 nanoparticles were synthesized by a typical procedure [20], 0.25 g of CTAB, 1.7 g of F127, 17.0 g of ethanol, 48.0 mL of deionized (DI) water and 5.0 g of 25–28 wt% NH_4OH solution were mixed to obtain a clear solution at 30 °C. Then, 0.9 g of TEOS was immediately added to the reaction solution with stirring at 1000 rpm for 1 min. After that, the reaction mixture was allowed to stand for 24 h without stirring. The white solid product was recovered through ultrahigh speed centrifuge and was washed with DI water for 3 times, then dried at 70 °C in air. Finally, the solid product was calcined at 550 °C for 5 h in air to remove the surfactants.

ZIF-8 nanoparticles were prepared in aqueous solution [21]. $\text{Zn}(\text{NO}_3)_2 \cdot 6\text{H}_2\text{O}$ (0.59 g) and 2-methylimidazole (11.35 g) were dissolved in 4.0 mL and 40.0 mL of DI water, respectively. Then, the two solutions were mixed under stirring and it turned milky almost instantly. After stirring for 5 min, the product was collected through ultrahigh speed centrifuge and washed with DI water. All the synthesis procedures were performed at room temperature.

2.3. Fabrication of nanoparticles incorporated TFN membranes

The TFN membrane was prepared via the interfacial polymerization of MPD with TMC by dispersing nanofillers into the aqueous solution of 2% w/v MPD and 0.15% w/v SDS and/or in the hexane solution of 0.1% w/v TMC simultaneously/singly. Hydrophilic MCM-48 and hydrophobic ZIF-8 were used as the nanofillers to fabricate the TFN membranes, respectively. The MPD solution was first poured on the surface of polysulfone support and maintained for 2 min. Then, the excessive MPD solution was drained and the soaked polysulfone support was dried in air for 9 min. Then, the TMC solution was poured on the surface of the soaked polysulfone support and allowed to be contacted for 1 min. The excessive TMC solution was removed and the resulting membrane was cured in the oven at 115 °C for 3 min to ensure complete polymerization. The resulting membranes were rinsed with DI water and stored in DI water.

The resultant membranes are designated as TFC for the pristine PA TFC membrane without nanoparticles; TFN-M-O and TFN-M-A for the membranes with dispersing MCM-48 totally in TMC organic phase singly and in MPD aqueous phase singly, respectively; TFN-Z-O and TFN-Z-A for the membranes with dispersing ZIF-8 totally in TMC organic phase singly and in MPD aqueous phase singly, respectively. TFN-M-OA was noted for the membrane with dispersing MCM-48 nanoparticles in TMC organic phase and MPD aqueous phase simultaneously. And TFN-Z-OA was noted for the membrane prepared with the both TMC organic phase and MPD aqueous phase containing ZIF-8 nanoparticles. The nanofillers compositions in the aqueous phase and/or organic phase solution of the samples are given in Table 1.

2.4. Characterization methods

Scanning electron microscope (SEM) (Hitachi S-4800, Japan) was used to characterize the morphology of the samples. Samples were deposited on sample holders with adhesive carbon foil and were sputtered with gold before measurement. The SEM equipped with an energy-dispersive X-ray detector (EDX) was utilized to conduct elemental mapping. The XRD of samples were recorded on a Bruker D8 ADVANCE instrument equipped with a Cu $\text{K}\alpha$ radiation at the rate of 1°/min. To characterize the hydrophilicity of the resultant membranes, the sessile drop contact angles of the membranes were performed by a contact angle analyzer DSA 100 (Kruss, Germany). The equilibrium value was the steady-state average of left and right angles. The data reported were the average of eight measurements for each membrane sample.

Table 1
Nanofillers composition in the aqueous phase and/or organic phase of the polyamide membranes prepared

Sample ^a	MCM-48 (%w/v)		ZIF-8 (%w/v)		Total amount of nanofiller (% w/v) ^b
	Organic phase	Aqueous phase	Organic phase	Aqueous phase	
TFC	–	–	–	–	0.0
TFN-M-O1	0.005	–	–	–	0.005
TFN-M-O2	0.010	–	–	–	0.010
TFN-M-A1	–	0.005	–	–	0.005
TFN-M-A2	–	0.010	–	–	0.010
TFN-M-OA	0.005	0.005	–	–	0.010
TFN-Z-O1	–	–	0.025	–	0.025
TFN-Z-O2	–	–	0.050	–	0.050
TFN-Z-O3	–	–	0.075	–	0.075
TFN-Z-A1	–	–	–	0.025	0.025
TFN-Z-A2	–	–	–	0.050	0.050
TFN-Z-OA1	–	–	0.025	0.025	0.050
TFN-Z-OA2	–	–	0.050	0.025	0.075

^aFor all the samples MPD and TMC are kept as 2% w/v and 0.1% w/v, respectively.

^bThe total amount of nanofillers were added during the interfacial polymerization process of preparation of each sample.

2.5. Reverse osmosis performance

The RO desalination performance of the synthesized membranes were evaluated using across-flow permeation apparatus. The test was conducted with an effect area of 19.6 cm² and a 2,000 ppm NaCl solution at 20°C and operating pressure of 16 bar.

The water flux F (L/m²h) was calculated by measuring the water permeability volume Q (L) through the membrane with effective surface area A (m²) over a period of time t (h).

$$F = \frac{Q}{At} \quad (1)$$

The salt rejection R (%) was determined as

$$R(\%) = \left(1 - \frac{C_p}{C_f}\right) \times 100 \quad (2)$$

where C_f and C_p (ppm) represent salt concentrations in the feed and permeate solutions, respectively, which were determined by a conductivity meter.

3. Results and discussion

3.1. Characterization of the nanoparticles

Fig. 1 shows the SEM images of the prepared MCM-48 and ZIF-8 nanoparticles. The prepared MCM-48 nanoparticles possess of monodispersed spherical shape (Fig. 1a) with the average particle size of 128 nm determined from the particle diameter distribution (Fig. 1b). The prepared ZIF-8 nanoparticles possess of polyhedral structure (Fig. 1c) with the average particle size of 178 nm determined from the particle diameter distribution (Fig. 1d). The pore structure of the synthesized nanoparticles is characterized

by XRD, and the patterns are shown in Fig. 2. The MCM-48 exhibits typical diffraction peaks indexed as planes (211) and (220) corresponding to the 3-D cubic space group (Fig. 2a). This finding confirms that the synthesized nanosphere is MCM-48-type mesoporous silica with a highly ordered mesoporous structure [22]. XRD pattern of ZIF-8 (Fig. 2b) shows high similarity with the result reported in literature [21] which confirms the formation of well-crystalline pure ZIF-8.

3.2. The novel TFN membrane prepared with MCM-48 nanoparticles

3.2.1. Characterization of the TFN-M membranes containing MCM-48

Fig. 3 shows the SEM images of the surface TFC and TFN-M membranes formed with different adding method and amount of MCM-48 nanoparticles. As clearly seen, the SEM image of the pristine TFC membrane (Fig. 3a) exhibits the typical “ridge-and-valley” structure of polyamide layer fabricated via interfacial polymerization of TMC and MPD. The TFN-M-O1 (Fig. 3b) and TFN-M-O2 (Fig. 3c) membranes synthesized by dispersing MCM-48 in TMC organic phase with 0.005% (w/v) and 0.01% (w/v), respectively, appear to have “leaf-like” morphological structure. It is due to that the hydrophilic nanoparticles in the organic phase strengthens the miscibility of the organic phase and aqueous phase during the formation of polyamide layer, leading to form the “leaf-like” structure [3]. The surface structure of TFN-M-A1 (Fig. 3d) and TFN-M-A2 (Fig. 3e) membranes formed by dispersing 0.005% (w/v) and 0.01% (w/v) of MCM-48 in MPD aqueous phase respectively, are similar with pristine TFC (Fig. 3a). Our previous study results indicate that the nanofillers would be embedded throughout the polyamide layer for the TFN membranes fabricated

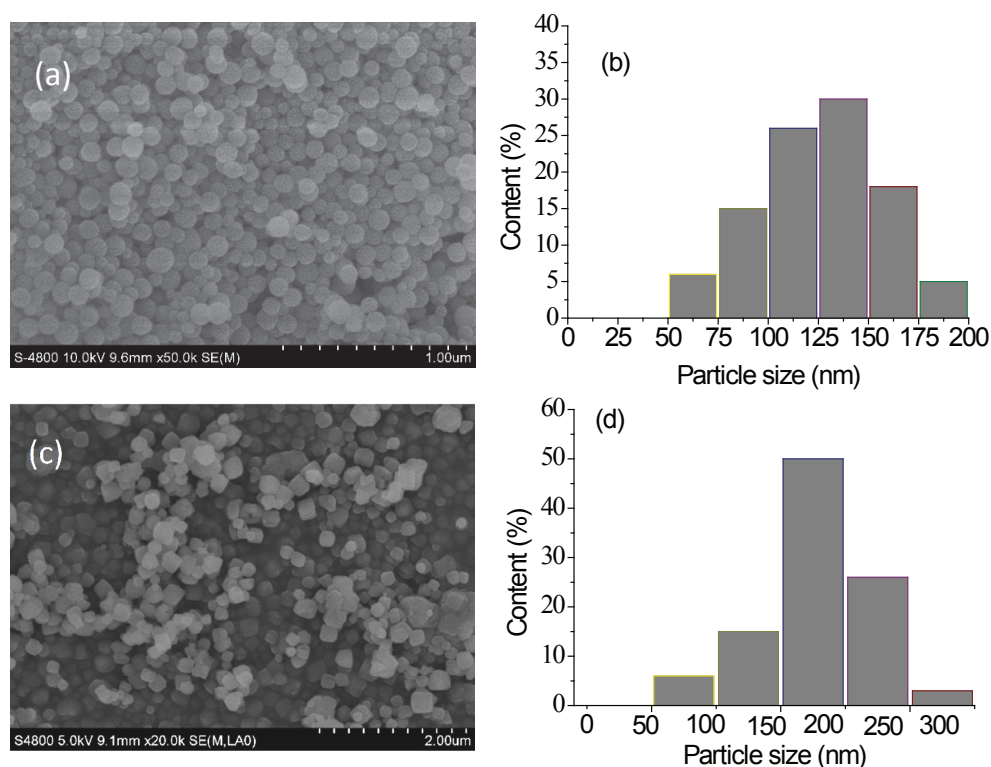


Fig. 1. SEM images for the morphology of (a) MCM-48 and (c) ZIF-8, and corresponding particle diameter distribution of (b) MCM-48 and (d) ZIF-8.

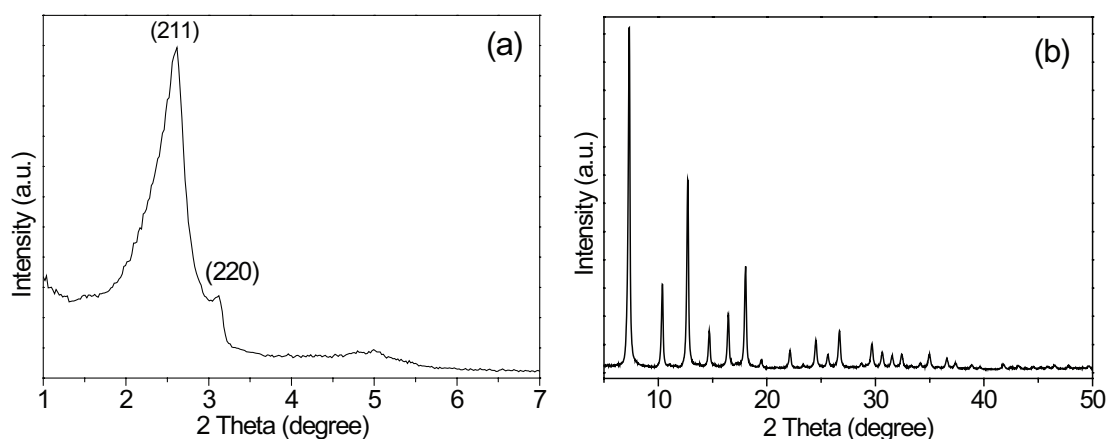


Fig. 2. XRD patterns of the prepared nanoparticles of MCM-48 (a) and ZIF-8 (b).

by dispersing the nanofillers in the TMC organic phase, because of the nanoparticles consist in the polymerization reaction zone during the interfacial polymerization process [19]. Whereas, the majorities of the nanofillers reside at the interface of the polysulfone support and polyamide layer due to the nanofillers pre-deposited on the polysulfone support which under the polymerization reaction zone. Therefore, the MCM-48 dispersing in aqueous phase has slightly influence on the surface morphology structure of polyamide layer than that in organic phase. It is believed that the nanostructure of the polyamide layer of the TFC membrane is asymmetric with a loose phase on the surface side and a

dense phase on the support side. Therefore, the nanoparticles changes the structure of the polyamide loose phase by dispersing in organic phase, and changes the structure of the polyamide dense phase by dispersing in aqueous phase. The surface morphology of the TFN-M-OA membrane fabricated by dispersing 0.005% w/v of MCM-48 in organic phase and 0.005% w/v of MCM-48 in aqueous phase (Fig. 3f) is similar with TFN-M-O1 membrane (Fig. 3b). Figs. 3 g–i show the SEM images of the surface toward the polysulfone support of isolated polyamide thin layer peeled from the polysulfone support by dissolving polysulfone with dichloromethane. It can be seen that the surface

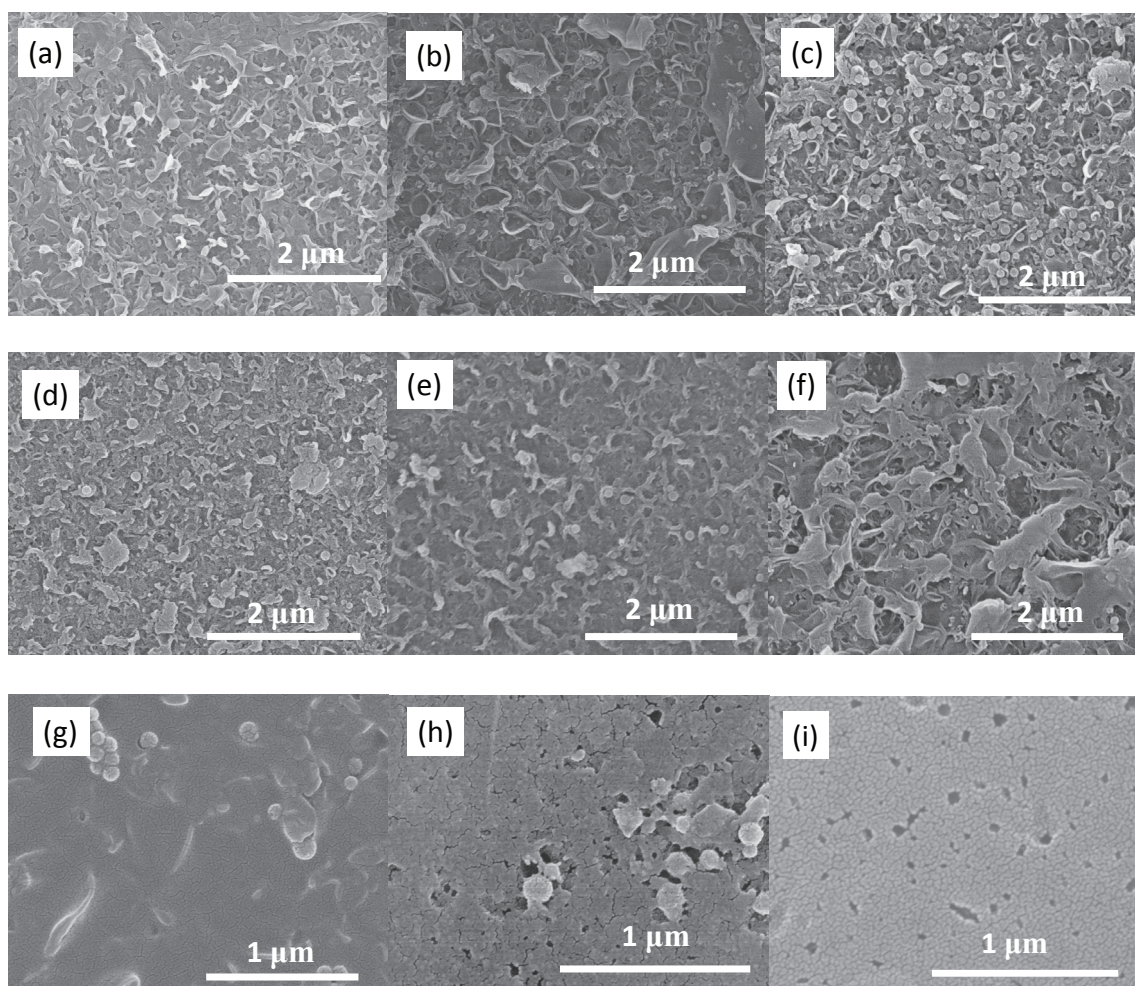


Fig. 3. SEM images for the surfaces of (a) the pristine TFC membrane and TFN-M membranes prepared with dispersing MCM-48 nanoparticles totally into TMC organic phase singly (b) TFN-M-O1 (0.005% w/v), (c) TFN-M-O2 (0.01% w/v), totally into MPD aqueous phase singly (d) TFN-M-A1 (0.005% w/v), (e) TFN-M-A2 (0.01% w/v), and partial into TMC organic phase and partial into MPD aqueous phase simultaneously (f) TFN-M-OA (0.005% w/v in organic phase and 0.005% w/v in aqueous phase); and the surfaces toward polysulfone support of the isolated polyamide thin layer peeled from polysulfone support (g) TFN-M-O1, (h) TFN-M-A1, and (i) TFN-M-OA.

toward the polysulfone support of TFN-M-O1 membrane (Fig. 3g) is dense and the embedded spherical shape can be observed. Whereas, lots of large pores were found on the surface toward the polysulfone support of TFN-M-A1 membrane (Fig. 3h), indicating low crosslinking of the TFN membrane fabricated with nanoparticles in aqueous phase. The surface toward the polysulfone support of TFN-M-OA membrane (Fig. 3i) is porosity similar with TFN-M-A1 membrane (Fig. 3h). The SEM images (Figs. 3f and 3i) show that the TFN-M-OA membrane (fabricated by dispersing 0.005% w/v of MCM-48 in organic phase and 0.005% w/v of MCM-48 in aqueous phase) has similar surface morphology with TFN-M-O1 (Fig. 3b) (fabricated by dispersing 0.005% w/v of MCM-48 in organic phase), and has similar surface toward the polysulfone support with TFN-M-A1 membrane (Fig. 3h) (formed by dispersing 0.005% (w/v) of MCM-48 in MPD aqueous phase). It indicates that the loose phase on the surface side and dense phase on the support side of the polyamide layer of TFN-M-OA membrane were

both modified by the nanoparticles dispersed in organic phase and aqueous phase. Therefore, the structure of the polyamide layer of TFN membrane prepared with simultaneous dispersion of nanoparticles in aqueous phase and organic phase can combine the benefits of the TFN membranes prepared by dispersing nanoparticles in organic phase singly and that in aqueous phase singly.

Fig. 4 presents the SEM images of the cross-section of the TFC and TFN-M membranes. Notably, a dense PA active film formed on top of the polysulfone substrate for all the membranes. Images (Figs. 4 b–f) show the larger “ridge-and-valley” on the surface of the TFN-M membranes, which is consistent with the “leaf-like” morphological structure.

The hydrophilicity of membrane surface was determined by measuring the water contact angle. The water contact angle of the pristine TFC and TFN-M membranes incorporated with MCM-48 are shown in Fig. 5. The contact angles of the TFN-M-O1 and TFN-M-O2 mem-

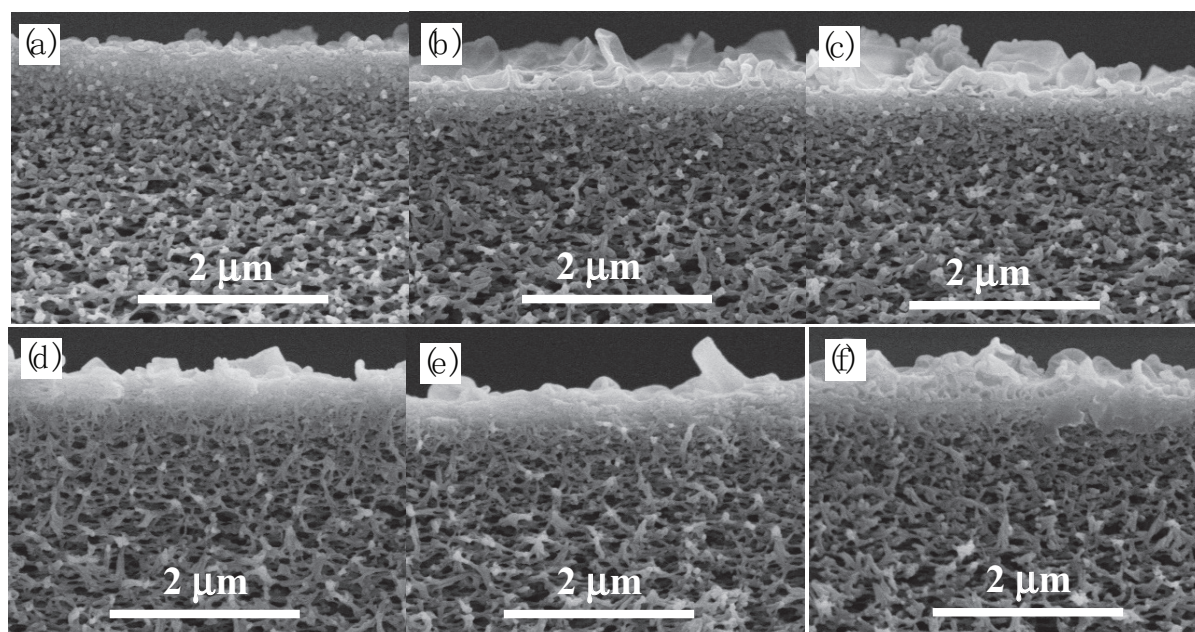


Fig. 4. SEM images for the cross-section of the pristine TFC membrane (a) and TFN-M membranes prepared with dispersing MCM-48 nanoparticles totally into TMC organic phase singly (b) TFN-M-O1 (0.005% w/v), (c) TFN-M-O2 (0.01% w/v), totally into MPD aqueous phase singly (d) TFN-M-A1 (0.005% w/v), (e) TFN-M-A2 (0.01% w/v), and partial into TMC organic phase and partial into MPD aqueous phase simultaneously (f) TFN-M-OA (0.005% w/v in organic phase and 0.005% w/v in aqueous phase).

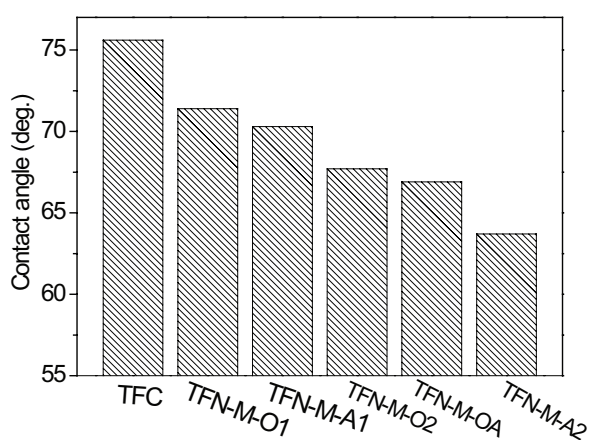


Fig. 5. Contact angles changes of the pristine TFC and TFN-M membranes prepared with dispersing MCM-48 nanoparticles totally into TMC organic phase singly TFN-M-O1 (0.005% w/v), TFN-M-O2 (0.01% w/v), totally into aqueous phase singly TFN-M-A1 (0.005% w/v), TFN-M-A2 (0.01% w/v), and partial into TMC organic phase and partial into MPD aqueous phase simultaneously TFN-M-OA (0.005%w/v in organic phase and 0.005%w/v in aqueous phase).

branes reduced with the increase content of MCM-48 in the organic phase, indicating that the increase in hydrophilicity of the TFN membrane. The increase of hydrophilicity for the TFN-M-O membranes is contributed to the hydrophilic MCM-48 nanoparticles throughout the entire polyamide layer, which accelerated the spread of water molecules on the membrane surface heightened the hydrophilic nature of the membrane and enhanced [19].

The contact angles of the TFN-M-A1 and TFN-M-A2 membranes decreased with the increase of MCM-48 nanoparticles content in the MPD aqueous phase, indicating the enhanced hydrophilicity of the TFN-M-A membranes. The increased hydrophilicity of the TFN-M-A membranes fabricated by dispersing MCM-48 into the aqueous phase is mainly contributed to lower crosslinking content of TFN membrane [6]. Therefore, more carboxylic acid groups were exposed on the surface, contributing to the reduced water contact angle. The SEM image (Fig. 3b) with porosity surface of the TFN-M-A1 membrane can confirm the low crosslinking content. The contact angle of TFN-M-OA membrane intermediated between TFN-M-O2 and TFN-M-A2, although the same total amount of MCM-48 were added before the interfacial polymerization for the above three membranes (Table 2). It further proves that the nanoparticles has different influence when it was dispersed in different phase, which is consistent with the surface structure of the membranes (Fig. 3).

The influence of MCM-48 nanoparticle loadings and adding mode on the membrane separation performance in terms of water flux and salt rejection were investigated at 16 bar and room temperature with 2,000 ppm NaCl as a feed solution, and the results are listed in Table 2. The water flux of TFN-M membranes enhanced with the increase in MCM-48 loading in TMC organic phase or MPD aqueous phase singly. The increase of the water flux is attributed to the enhanced hydrophilicity of the resultant membranes and the lower crosslinking of the polyamide layer due to the role of the MCM-48 nanoparticles. The salt rejection of TFN-M-A membranes is smaller than that of TFN-M-O membranes. It is due to that the nanoparticles in TFN-M-A membranes changed the polyamide dense phase which acts as the true separation barrier resulting decrease in

Table 2

Effect of MCM-48 loading and the adding mode on separation performance of membranes fabricated with MCM-48 nanoparticles singly in organic phase (TFN-M-O) and aqueous phase (TFN-M-A), and simultaneously in two phases (TFN-M-OA)

Sample	Total amount of MCM-48 (%w/v) ^a	F (L/m ² h)	Increased F (L/m ² h) ^c	R (%)
TFC	0.0	16.6	–	97.5
TFN-M-O1	0.005	32.7	16.1	97.7
TFN-M-O2	0.010	37.4	20.8	98.6
TFN-M-A1	0.005	29.6	13.0	96.0
TFN-M-A2	0.010	32.8	16.2	93.8
TFN-M-OA	0.010 ^b	43.7	27.1	97.0

^aThe total amount of MCM-48 were added during the interfacial polymerization process of preparation of each sample.

^bIn TFN-M-OA, the total amount of MCM-48 of 0.010% (w/v) was added by dispersing 0.005% (w/v) in organic phase and 0.005% w/v in aqueous phase.

^cThe value is increased water flux of the TFN membrane compared with the pristine TFC membrane in the first row.

salt rejection [5,23]. The water flux of TFN-M-OA is higher than the TFN membrane prepared with total amount of MCM-48 in singly phase in the literature [19] and the salt rejection are all over 97%.

As shown in Table 2, the increased water flux value of TFN-M-OA membrane compared with pristine TFC membrane is nearly the sum that of the TFN-M-A1 and TFN-M-O1 membrane (fourth row in Table 2). And the high salt rejection of TFN-M-OA membrane is similar with TFN-M-O1 and TFN-M-A1 membrane. The interesting results indicate that for TFN-M-OA membrane the nanoparticles (0.005% w/v) dispersed in aqueous phase change the structure of the dense phase on the support side of the polyamide layer similar with TFN-M-A1 membrane and the nanoparticles (0.005% w/v) dispersed in organic phase change the structure of the loose phase on the surface side of the polyamide layer similar with TFN-M-O1 membrane. Therefore, the increase of water flux value of TFN-M-OA membrane is nearly the sum that of the TFN-M-A1 and TFN-M-O1 membrane, and the salt rejection is still high similar with the TFN-M-A1 and TFN-M-O1 membrane. And, the TFN-M-OA membrane possesses higher water flux than TFN-M-O2 and TFN-M-A2 membrane prepared with same total amount MCM-48 nanoparticles in single phase. For the reported TFN membranes, the water flux increased sharply with increasing nanofillers loadings when less amount nanofillers was added, however, the water flux increases slowly with further increase of nanofillers at higher content. It is believed that it is difficult to uniform disperse the nanofillers of high content in the solution and aggregation will be occurred at higher nanofillers concentration. Therefore, the enhancement degree of nanoparticles on membrane performance is not directly proportional to the content of nanoparticles. It indicates that it is feasible to fabricate the TFN membrane with enhanced performance by simultaneously dispersing the less amount of nanofillers in organic and aqueous phases to control the polyamide asymmetric dense phase and loose phase simultaneously. Furthermore, the new strategy is realized by dispersing less amount nanofillers in both phases at the same time, which is possible to avoid the aggregation of nanoparticles and maximize the effect of nanoparticles.

3.2.2. Chlorine resistance of the TFN-M RO membranes

The chlorine stability of the resultant membrane was evaluated by soaking the membrane sample in sodium hypochlorite (NaClO) aqueous solution to investigate the changes of water flux and salt rejection after treatment. In the chlorine exposure test, membrane sample was exposed to 100 ppm NaClO aqueous solution at pH 7.0 and 20 °C for 1, 5, 10, 20 and 80 h, respectively. The total chlorine exposures of the chlorinated membranes were 100, 500, 1,000, 2,000 and 8,000 ppm h NaClO, respectively. The chlorine treated membranes were thoroughly rinsed with deionized water, and reloaded in the test cell. The water flux and salt rejection of the membranes were tested again with 2,000 ppm NaCl aqueous solution.

The variations of water flux and salt rejection of the membranes with total chlorine exposure of ppm h NaClO at pH 7.0 are shown in Fig. 6. With the increasing total chlorine exposure, a significant increase of water flux and a sharp decline of salt rejection occurred for the pristine TFC membrane, while the variations of water flux and salt rejection of the TFN membranes are relatively slow, indicating that the MCM-48 incorporated TFN membranes possess better chlorine stability than the pristine TFC membrane. The variations of water flux (increase) and salt rejection (decrease) after chlorine exposure are due to the N-chlorination reaction and ring-chlorination reaction via orton-rearrangement of aromatic polyamide chains during which the partially positively charged active chlorine species attack the active site in MPD residual, amide nitrogen or amide aromatic ring [18]. Therefore, the chlorination can destroy the symmetry of polyamide network by disrupting the intermolecular hydrogen bonds, which cause a conformational deformations of polyamide chains [24]. The chlorine resistance of the TFN-M membranes incorporated with MCM-48 nanoparticles are consistent with the hydrophilicity of the TFN membrane. Therefore, the chlorine resistance of TFN membranes can be attributed to the enhanced hydrophilicity [12]. As shown in Fig. 6, the TFN-M-AO, TFN-M-A and TFN-M-O membranes have similar chlorine stability. Therefore, it is possibility to improve the chlorine resistance of the polyamide membrane via the simple and feasible strategy by incorporating the MCM-

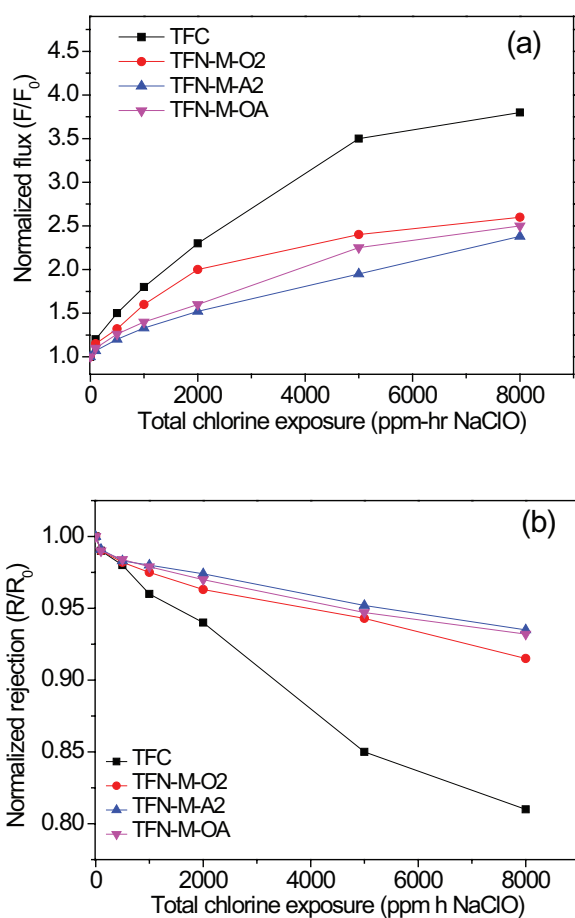


Fig. 6. Normalized water flux (a) and salt rejection (b) with total chlorine exposure of the prepared pristine TFC and TFN-M RO membrane after chlorination with 100 ppm NaClO solution at 20 °C and pH 7.0 and tested with 2,000 ppm NaCl under 16 bar.

48 nanoparticles dispersed in organic and/or aqueous phase simultaneously or singly.

3.2.3. Stability of the TFN-M RO membranes

The modified TFN membranes separation performance were investigated for long-term stability at the operating pressure of 16 bar for 120 h with 2,000 ppm NaCl aqueous solution. The TFN-M-O2, TFN-M-A2 and TFN-M-OA membranes were used for the long-term test experiments compared with pristine TFC membrane. The preparation conditions of the above membranes are listed in Table 1. The water flux and salt rejection of the membranes are shown in Fig. 7. It can be seen that the separation performances of the TFN-M-O2, TFN-M-A2 and TFN-M-OA membranes are stable in terms of water flux and salt rejection. The results indicate that the MCM-48 nanoparticles can stably reside in the resultant TFN membranes whether the nanoparticles were dispersed singly into organic phase, or aqueous phase, or simultaneously into the two phases. Therefore, the TFN RO membrane prepared via the new strategy by dispersing nanoparticles in the organic and aqueous phases simultaneously of interfacial polymerization possess better

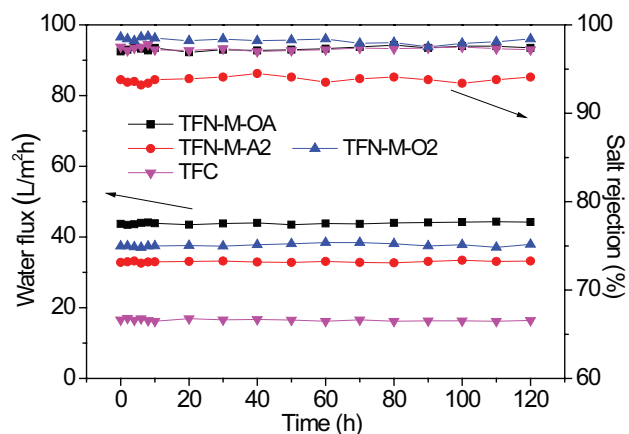


Fig. 7. Stability of the resultant TFC and TFN-M membranes during 120 h test with 2,000 ppm NaCl aqueous solution at 16 bar and 20 °C.

separation performance with higher water flux and similar salt rejection and stability than the membrane prepared by dispersing nanoparticles in singly phase.

3.3. The novel TFN membrane prepared with ZIF-8 nanoparticles

3.3.1. Characterization of the TFN-Z RO membranes containing ZIF-8

In order to test the practicability of the new strategy, hydrophobic ZIF-8 nanoparticles was used as nanofillers to prepare the TFN RO membranes. The preparation conditions of the membranes are listed in Table 1. Fig. 8 shows the SEM images of the surface of TFC and TFN-Z membranes formed with different adding method and amount of ZIF-8 nanoparticles. The TFN-Z-O1 membrane prepared by dispersing 0.025% (w/v) ZIF-8 in organic phase has a flatter morphology with shorter ridges and shallower valleys (Fig. 8b) than the pristine polyamide TFC membrane with the typical “ridge-and-valley” structure (Fig. 8a). With increasing the loading of ZIF-8 to 0.05% (w/v), the surface of TFN-Z-O2 has become rough and traditional nodular structure (Fig. 8c). Figs. 8d and 8e show the surface SEM images of the TFN-Z-A1 and TFN-Z-A2 membranes prepared by dispersing 0.025% (w/v) and 0.05% (w/v) of ZIF-8 in aqueous phase, respectively. The surface morphology of the TFN-Z-OA1 membrane (Fig. 8f) and TFN-Z-OA2 membrane (Fig. 8g) is similar with TFN-Z-O1 membrane (Fig. 8b) and TFN-Z-O2 membrane (Fig. 8c). The changing trend of TFN-Z membrane is the same with TFN-M membrane.

Fig. 9 presents the SEM images of the cross-section of the TFC and TFN-Z membranes. Notably, a dense PA active film formed on top of the polysulfone substrate for all the membranes. Images (Figs. 9 b–h) show the larger “ridge-and-valley” on the surface of the TFN-Z membranes, which is consistent with the “leaf-like” morphological structure. The changing trend of TFN-Z membrane is the same with the TFN-M membrane.

The effect of ZIF-8 nanoparticle loadings and adding mode on membrane separation performance in terms of

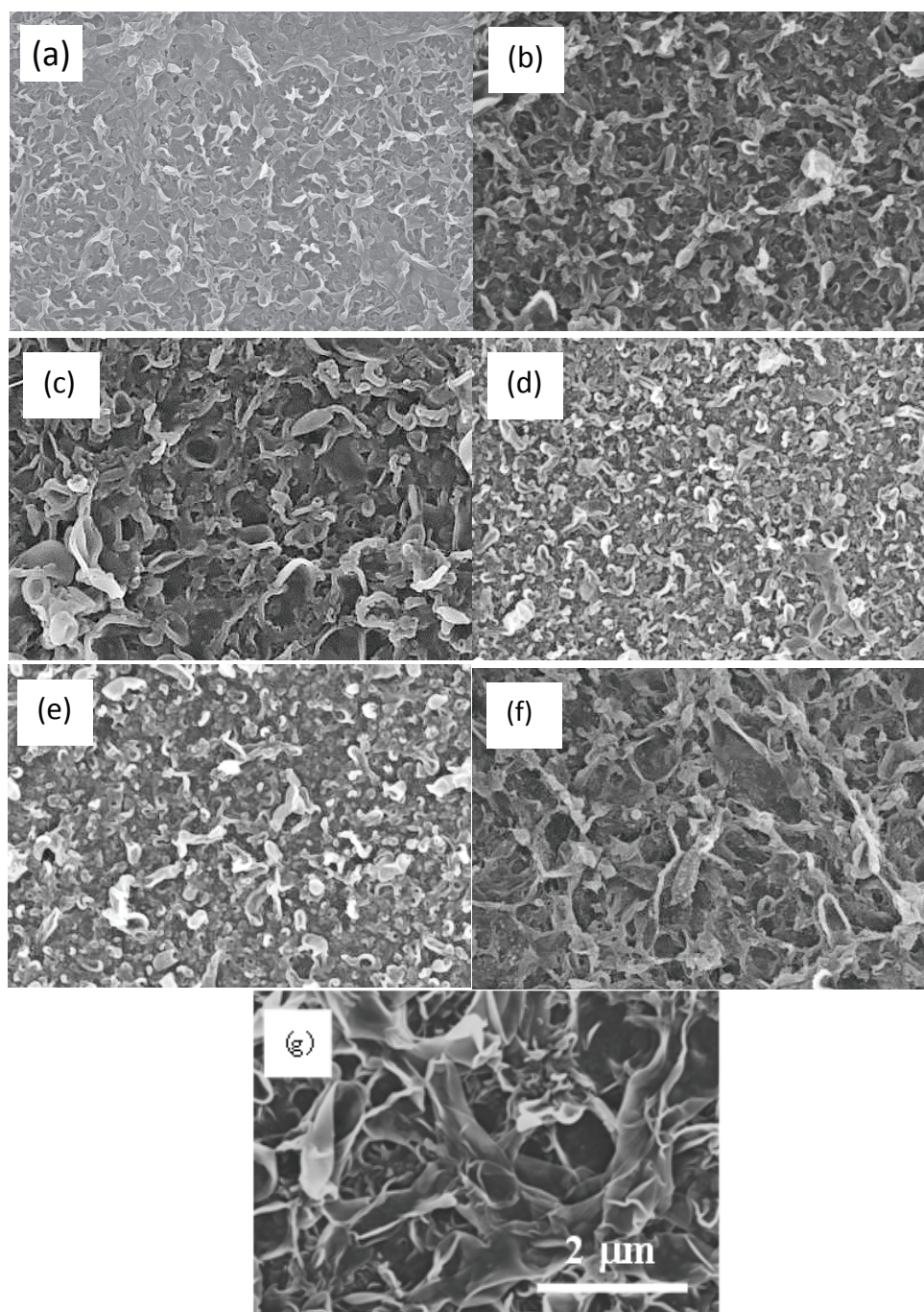


Fig. 8. SEM images for the surfaces of (a) pristine TFC membrane and TFN-Z membranes fabricated by dispersing ZIF-8 nanoparticles totally in organic phase singly (b) TFN-Z-O1 (0.025% w/v), (c) TFN-Z-O2 (0.050% w/v), totally in aqueous phase singly (d) TFN-Z-A1 (0.025% w/v) and (e) TFN-Z-A2 (0.050% w/v), and in organic phase and aqueous phase simultaneously (f) TFN-Z-OA1 (0.025% w/v in organic phase and 0.025% w/v in aqueous phase) and (g) TFN-Z-OA2 (0.05% w/v in organic phase and 0.025% w/v in aqueous phase).

water flux and salt rejection was investigated at 16 bar and room temperature with 2,000 ppm NaCl as a feed solution, and the results are listed in Table 3. The water flux of TFN-Z-O membranes enhanced with the increase in ZIF-8 content from 0.025% to 0.075% in organic phase, and the salt rejection keeps over 95.8%. When less amount of ZIF-8 nanoparticles (0.025%) were added in the aqueous phase, the water

flux of TFN-Z-A1 membrane increase and the salt rejection is 98%. However, the water flux sharply increase and the salt rejection reduce to 91.8% for the TFN-Z-A2 membrane when 0.05% of ZIF-8 nanoparticles were added in aqueous phase. It is due to that the nanoparticles change the structure of the polyamide loose phase by dispersing in organic phase, and changes the structure of the polyamide dense

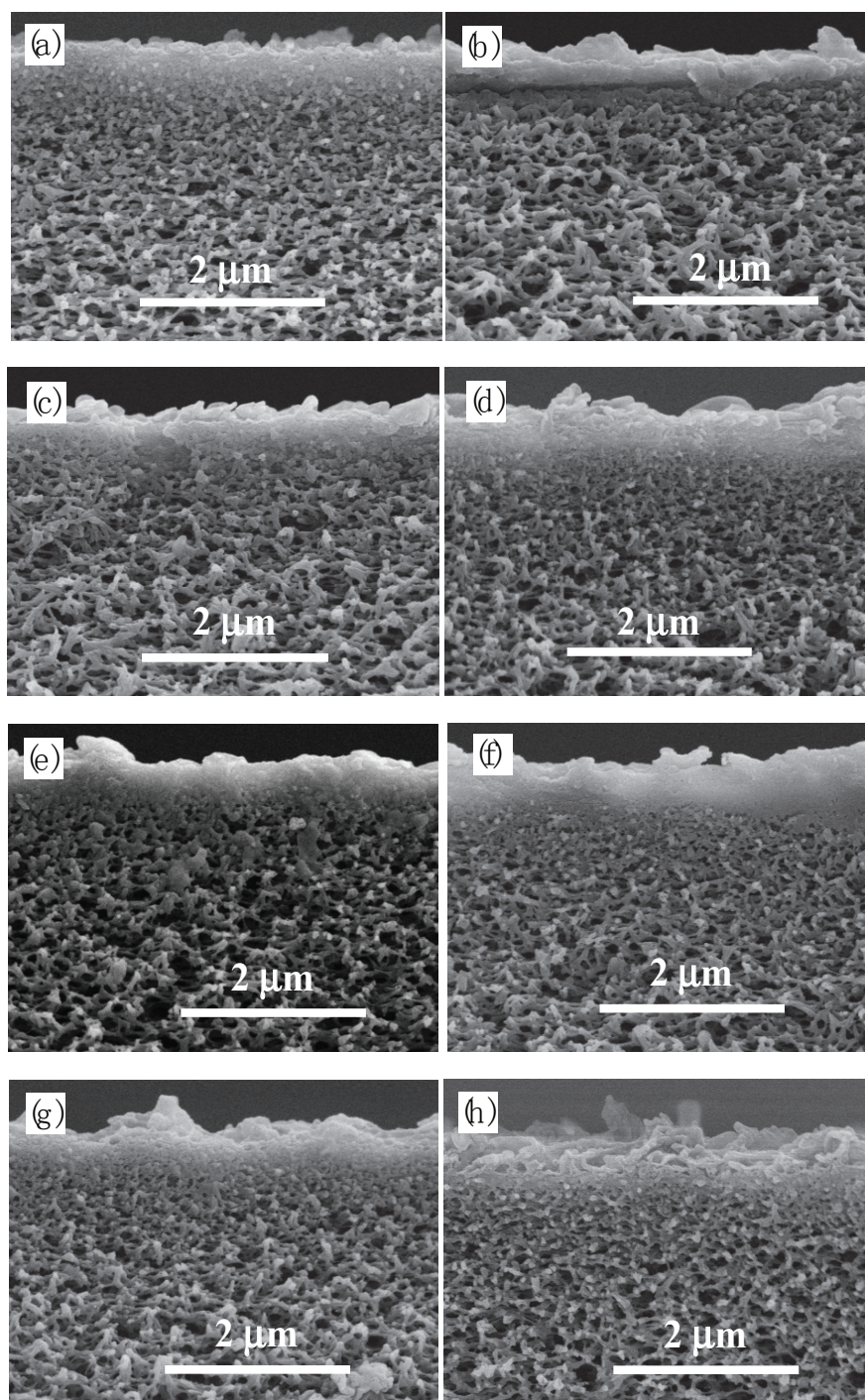


Fig. 9. SEM images for the cross-section of pristine TFC membrane (a) and TFN-Z membranes fabricated by dispersing ZIF-8 nanoparticles totally in organic phase singly (b) TFN-Z-O1 (0.025% w/v), (c) TFN-Z-O2 (0.050% w/v), (d) TFN-Z-O3 (0.075% w/v), totally in aqueous phase singly (e) TFN-Z-A1 (0.025% w/v) and (f) TFN-Z-A2 (0.050% w/v), and in organic phase and aqueous phase simultaneously (g) TFN-Z-OA1 (0.025% w/v in organic phase and 0.025% w/v in aqueous phase) and (h) TFN-Z-OA2 (0.05% w/v in organic phase and 0.025% w/v in aqueous phase).

phase by dispersing in aqueous phase. Therefore, the salt rejection of TFN-Z-A membranes by dispersing of nanoparticles in aqueous phase were greater change than that dispersion in organic phase. The increased water flux value of TFN-Z-OA1 membrane to the pristine TFC membrane is

the sum that of the TFN-Z-A1 and TFN-Z-O1 membrane, and the salt rejection is still high similar with the TFN-Z-A1 and TFN-Z-O1 membrane. The TFN-Z-OA membrane has the higher water flux and higher salt rejection than TFN-Z-O2 membrane prepared with same total amount ZIF-8

Table 3

Effect of ZIF-8 loading and the adding mode on separation performance of membranes with ZIF-8 nanoparticles singly in organic phase (TFN-Z-O) and aqueous phase (TFN-Z-A), and simultaneously in two phases (TFN-Z-OA)

Sample	Total amount of ZIF-8 (%w/v) ^a	F (L/m ² h)	Increased F (L/m ² h) ^d	R (%)
TFC	0.0	16.6	–	97.5
TFN-Z-O1	0.025	21.0	4.4	97.9
TFN-Z-O2	0.050	23.0	6.4	98.0
TFN-Z-O3	0.075	27.2	10.6	95.8
TFN-Z-A1	0.025	22.1	5.5	98.0
TFN-Z-A2	0.050	29.6	13.0	91.8
TFN-Z-OA1	0.050 ^b	25.3	8.7	97.4
TFN-Z-OA2	0.075 ^c	31.6	15.0	96.2

^aThe total amount of ZIF-8 were added during the interfacial polymerization process of preparation of each sample.

^bIn TFN-Z-OA1, the total amount of ZIF-8 of 0.050% (w/v) was added by dispersing 0.025% (w/v) in organic phase and 0.025% w/v in aqueous phase.

^cIn TFN-Z-OA2, the total amount of ZIF-8 of 0.075% (w/v) was added by dispersing 0.050% (w/v) in organic phase and 0.025% w/v in aqueous phase.

^dThe value is increased water flux of the TFN membrane compared with the pristine TFC membrane in the first row.

nanoparticles in organic phase. Also, the TFN-Z-OA2 membrane has the higher water flux and salt rejection than TFN-Z-O3 membrane prepared with same total amount ZIF-8 nanoparticles in organic phase. And the increase of water flux value of TFN-Z-OA2 membrane to the pristine TFC membrane is the sum that of the TFN-Z-O2 and TFN-Z-A1 membrane, and the salt rejection is still high similar with the TFN-Z-O2 and TFN-Z-A1 membrane. It also indicates that it is feasible to fabricate the TFN membrane with excellent performance by simultaneously dispersing the less amount of nanofillers in organic and aqueous phases to control the polyamide asymmetric dense phase and loose phase simultaneously, which is similar with the result of TFN-M.

The results are also similar with the TFN membranes incorporated with MCM-48 and ZIF-8. It indicates that the strategy to fabricate the TFN membranes by dispersing less amount nanofillers in organic and aqueous phase simultaneously is feasible to obtain the TFN membrane with excellence separation performance (higher water flux and higher salt rejection) compared with the conventional method by dispersing nanofillers in singly phase.

3.3.2. Chlorine resistance of the TFN-Z RO membranes

The experiments of chlorine stability of the TFN-Z membranes are same with the TFN-M membranes. The variations of water flux and salt rejection of the membranes with total chlorine exposure of ppm h NaClO at pH 7.0 are shown in Fig. 10. With the increasing total chlorine exposure, a significant increase of water flux and a sharp decline of salt rejection occurred for the pristine TFC membrane, while the variations of water flux and salt rejection of the TFN-Z membranes are relatively slow, indicating that the ZIF-8 incorporated TFN membranes possess better chlorine stability than the pristine TFC membrane. The TFN-Z-AO, TFN-Z-A and TFN-Z-O membranes have similar chlorine stability. Therefore, it is possibility to improve the chlorine resistance of the polyamide membrane via the simple and

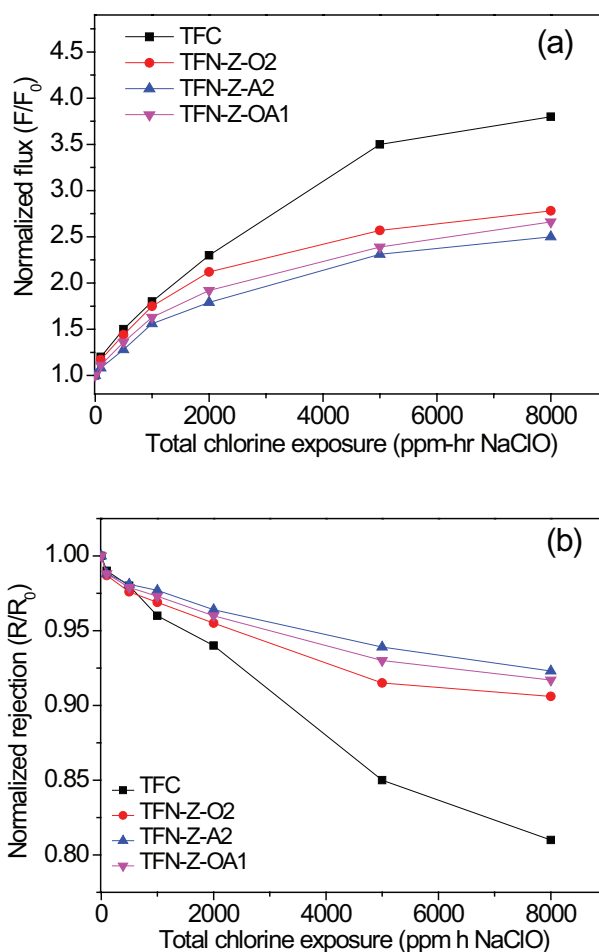


Fig. 10. Normalized water flux (a) and salt rejection (b) with total chlorine exposure of the prepared pristine TFC and TFN-Z RO membrane after chlorination with 100 ppm NaClO solution at 20 °C and pH 7.0 and tested with 2,000 ppm NaCl under 16 bar.

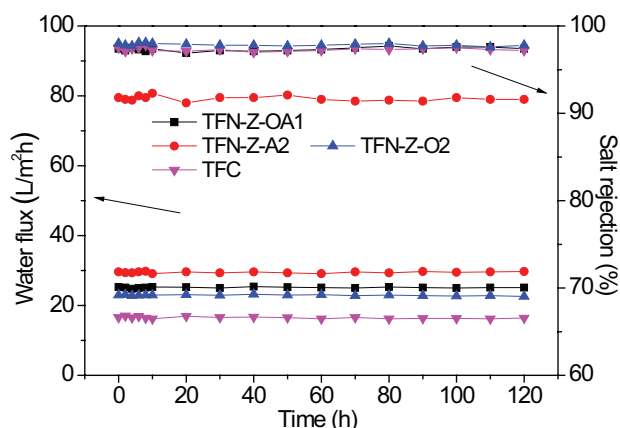


Fig. 11. Stability of the resultant TFC and TFN-Z membranes during 120 h test with 2,000 ppm NaCl aqueous solution at 16 bar and 20 °C.

feasible strategy by incorporating the ZIF-8 nanoparticles dispersed in organic and/or aqueous phase simultaneously or singly.

3.3.3. Stability of the TFN-Z RO membranes

The modified TFN membranes separation performance were investigated for long-term stability at the operating pressure of 16 bar for 120 h with 2,000 ppm NaCl aqueous solution. The TFN-Z-O2, TFN-Z-A2 and TFN-Z-OA1 membranes were used for the long-term test experiments compared with pristine TFC membrane. The preparation conditions of the above membranes are listed in Table 1. The water flux and salt rejection of the membranes are shown in Fig. 11. It can be seen that the separation performances of all the membranes are stable in terms of water flux and salt rejection. The results indicate that the ZIF-8 nanoparticles can stably reside in the resultant TFN-Z membranes whether the nanoparticles were dispersed singly into organic phase, or aqueous phase, or simultaneously into the two phases. Therefore, the TFN RO membrane prepared via the new strategy by dispersing nanoparticles in the organic and aqueous phases simultaneously of interfacial polymerization possess better separation performance with higher water flux and similar salt rejection and stability than the membrane prepared by dispersing nanoparticles in singly phase.

4. Conclusion

The nanoparticles incorporated thin film nanocomposite membrane has successfully been synthesized via interfacial polymerization method by dispersing the nanoparticles in organic phase and aqueous phase simultaneously. The new strategy allow the nanofillers to modify the structure of the loose phase and dense phase of polyamide layer simultaneously. The novel TFN membrane has the enhanced performance compared with the TFN prepared by dispersing the nanoparticles in singly phase with higher water flux and salt rejection. Furthermore, the new strategy is realized by dispersing less amount nanofillers in both phases at the same

time, which is possible to avoid the aggregation of nanoparticles and maximize the effect of nanoparticles. The hydrophilic MCM-48 and hydrophobic ZIF-8 nanoparticles can both enhanced the desalination performance by dispersed in organic phase and aqueous phase simultaneously, indicating that the new strategy has certain universality for nanomaterials with different properties to fabricate the TFN membrane. This method may also be applicable to the TFN membrane prepared by interfacial polymerization with different nanofillers not only for the RO application but also for NF and FO.

Acknowledgements

The financial support from the National Natural Science Foundation of China (No. U1607124, 21276246), Key Research Project of Shandong Province (No. 2017GHY215001) and the OUC-AU joint projects are gratefully acknowledged.

References

- [1] M. Elimelech, W.A. Phillip, The future of seawater desalination: energy, technology, and the environment, *Science*, 333 (2011) 712–717.
- [2] B.H. Jeong, E.M.V. Hoek, Y. Yan, A. Subramani, X. Huang, G. Hurwitz, A.K. Ghosh, A. Jawor, Interfacial polymerization of thin film nanocomposites: A new concept for reverse osmosis membranes, *J. Membr. Sci.*, 297 (2007) 1–7.
- [3] M.L. Lind, A.K. Ghosh, A. Jawor, X. Huang, W. Hou, Y. Yang, E.M.V. Hoek, Influence of zeolite crystal size on zeolite-polyamide thin film nanocomposite membranes, *Langmuir*, 25 (2009) 10139–10145.
- [4] M. Fathizadeh, A. Aroujalian, A. Raisi, Effect of added NaX nano-zeolite into polyamide as a top thin layer of membrane on water flux and salt rejection in a reverse osmosis process, *J. Membr. Sci.*, 375 (2011) 88–95.
- [5] H. Dong, L. Zhao, L. Zhang, H.L. Chen, C.J. Gao, W.S.W. Ho, High-flux reverse osmosis membranes incorporated with NaY zeolite nanoparticles for brackish water desalination, *J. Membr. Sci.*, 476 (2015) 373–383.
- [6] J. Yin, E. Kim, J. Yang, B.L. Deng, Fabrication of a novel thin-film nanocomposite (TFN) membrane containing MCM-41 silica nanoparticles (NPs) for water purification, *J. Membr. Sci.*, 423–424 (2012) 238–246.
- [7] E. Kim, B.L. Deng, Fabrication of polyamide thin-film nano-composite (PA-TFN) membrane with hydrophilized ordered mesoporous carbon (H-OMC) for water purifications, *J. Membr. Sci.*, 375 (2011) 46–54.
- [8] Q. Liu, G.R. Xu, Graphene oxide (GO) as functional material in tailoring polyamide thin film composite (PA-TFC) reverse osmosis (RO) membranes, *Desalination*, 394 (2016) 162–175.
- [9] M.R. Bao, G.R. Zhu, L. Wang, M. Wang, C.J. Gao, Preparation of monodispersed spherical mesoporous nanosilica-polyamide thin film composite reverse osmosis membranes via interfacial polymerization, *Desalination*, 309 (2013) 261–266.
- [10] G.R. Zhu, M.R. Bao, Z.F. Liu, C.J. Gao, Preparation of spherical mesoporous aminopropyl-functionalized MCM-41 and its application in polyamide thin film nanocomposite reverse osmosis membrane, *Desal. Water Treat.*, 57 (2016) 25411–25420.
- [11] J. Duan, Y. Pan, F. Pacheco, E. Litwiller, Z. Lai, I. Pinnau, High-performance polyamide thin-film-nanocomposite reverse osmosis membranes containing hydrophobic zeolitic imidazolate framework-8, *J. Membr. Sci.*, 476 (2015) 303–310.
- [12] M. Safarpour, A. Khataee, V. Vatanpour, Thin film nanocomposite reverse osmosis membrane modified by reduced graphene oxide/TiO₂ with improved desalination performance, *J. Membr. Sci.*, 489 (2015) 43–54.

- [13] A. Peyki, A. Rahimpour, M. Jahanshahi, Preparation and characterization of thin film composite reverse osmosis membranes incorporated with hydrophilic SiO₂ nanoparticles, *Desalination*, 368 (2015) 152–158.
- [14] L. Zhang, G.Z. Shi, S. Qiu, L.H. Cheng, H.L. Chen, Preparation of high-flux thin film nanocomposite reverse osmosis membranes by incorporating functionalized multi-walled carbon nanotubes, *Desal. Water Treat.*, 34 (2011) 19–24.
- [15] G.N.B. Baroña, J. Lim, M. Choi, B. Jung, Interfacial polymerization of polyamide-aluminosilicate SWNT nanocomposite membranes for reverse osmosis, *Desalination*, 325 (2013) 138–147.
- [16] D. Emadzadeh, W.J. Lau, M. Rahbari-Sisakht, A. Daneshfar, M. Ghanbari, A. Mayahi, T. Matsuura, A.F. Ismail, A novel thin film nanocomposite reverse osmosis membrane with superior anti-organic fouling affinity for water desalination, *Desalination*, 368 (2015) 106–113.
- [17] M. Ghanbari, D. Emadzadeh, W.J. Lau, T. Matsuura, A.F. Ismail, Synthesis and characterization of novel thin film nanocomposite reverse osmosis membranes with improved organic fouling properties for water desalination, *RSC Adv.*, 5 (2015) 21268–21276.
- [18] H.Y. Zhao, S. Qiu, L.G. Wu, L. Zhang, H.L. Chen, C.J. Gao, Improving the performance of polyamide reverse osmosis membrane by incorporation of modified multi-walled carbon nanotubes, *J. Membr. Sci.*, 450 (2014) 249–256.
- [19] L. Liu, G.R. Zhu, Z.F. Liu, C.J. Gao, Effect of MCM-48 nanoparticles on the performance of thin film nanocomposite membranes for reverse osmosis application, *Desalination*, 394 (2016) 72–82.
- [20] T.W. Kim, P.W. Chung, V.S.Y. Lin, Facile synthesis of monodisperse spherical MCM-48 mesoporous silica nanoparticles with controlled particle size, *Chem. Mater.*, 22 (2010) 5093–5104.
- [21] Y.C. Pan, Y.Y. Liu, G.F. Zeng, L. Zhao, Z.P. Lai, Rapid synthesis of zeolitic imidazolate framework-8 (ZIF-8) nanocrystals in an aqueous system, *Chem. Commun.*, 47 (2011) 2071–2073.
- [22] J.S. Beck, J.C. Vartuli, W.J. Roth, M.E. Leonowicz, C.T. Kresge, K.D. Schmitt, C.T.-W. Chu, D.H. Olson, E.W. Sheppard, S.B. McCullen, J.B. Higgins, J.L. Schlenker, A new family of mesoporous molecular sieves prepared with liquid crystal templates, *J. Am. Chem. Soc.*, 114 (1992) 10834–10843.
- [23] F.A. Pacheco, I. Pinnau, M. Reinhard, J.O. Leckie, Characterization of isolated polyamide thin films of RO and NF membranes using novel TEM techniques, *J. Membr. Sci.*, 358 (2010) 51–59.
- [24] G.D. Kang, C.J. Gao, W.D. Chen, X.M. Jie, Y.M. Cao, Y. Quan, Study on hypochlorite degradation of aromatic polyamide reverse osmosis membrane, *J. Membr. Sci.*, 300 (2007) 165–171.